Smart Structures and Systems, *Vol. 15, No. 3 (2015) 863-879*
DOI: http://dx.doi.org/10.12989/sss.2015.15.3.863

Experimental investigation of an active mass damper system with time delay control algorithm

Dong-Doo Jang[1], Jeongsu Park[2] and Hyung-Jo Jung[*2]

[1]*Korea Railroad Research Institute, Euiwang, Gyeonggi-do 437-757, Korea*
[2]*Department of Civil and Environmental Engineering, KAIST, Daejeon 305-701, Korea*

(Received November 27, 2014, Revised January 19, 2015, Accepted January 21, 2015)

Abstract. This paper experimentally investigates the effectiveness and applicability of the time delay control (TDC) algorithm, which is simple and robust to unknown system dynamics and disturbance, for an active mass damper (AMD) system to mitigate the excessive vibration of a building structure. To this end, the theoretical background including the mathematical formulation of the control system is first described; and then, a thorough experimental study using a shaking table system with a small-scale three-story building structural model is conducted. In the experimental tests, the performance of the proposed control system is examined by comparing its structural responses with those of the uncontrolled system in the free vibration and forced vibration cases. It is clearly verified from the test results that the TDC algorithm embedded AMD system can effectively reduce the structural response of the building structure.

Keywords: time delay control algorithm; unknown dynamics; vibration mitigation; active mass damper; shaking table test

1. Introduction

One of the widely used control strategies for mitigating excessive vibration of building structures having low inherent damping ratios is to introduce inertial control-type dampers (e.g., tuned mass damper (TMD), active mass damper (AMD), etc.) to the structures. Since the AMD system has several attractive features such as high control efficiency, good adaptability and relative insensitivity to site conditions compared to the TMD system, it can be considered as an effective means for response reduction of high-rise building structures subjected to dynamic loadings like earthquakes and winds, especially small-to-medium earthquakes and strong winds. The AMD system was first applied to a full-scale building structure 25 years ago (Kobori *et al*. 1991a, b). Since then, this type of the active control system has been implemented in more than 40 buildings (Nishitani and Inoue 2001, Spencer and Nagarajaiah 2003).

Successful operation of the AMD system is highly dependent upon an embedded control algorithm in the control system. For the AMD system, a lot of control algorithms (e.g., control algorithms based on linear optimal control theory such as LQG and H2, sliding mode control algorithm, adaptive control algorithm, intelligent control algorithms such as neural network-based

*Corresponding author, Associate Professor, E-mail: hjung@kaist.ac.kr

http://www.techno-press.org/?journal=sss&subpage=8 ISSN: 1738-1584 (Print), 1738-1991 (Online)

control and fuzzy logic-based control, etc.) have been studied (Datta 2001, Dyke *et al*. 1996, Pourzeynali *et al*. 2007). However, most of the algorithms have been originally developed in other engineering fields (e.g., electrical or mechanical engineering); so sometimes they might not fit very well with large-scale civil engineering structures such as bridges and buildings. For example, the most popular LQG and H2 algorithms require an exact mathematical model of a structure of interest, but it is too difficult to know a precise mathematical model of a large civil structure due to its complexity and uncertainty. Moreover, civil structures have slow dynamics; in other words, their dominant natural frequencies are relatively low compared to structural systems in mechanical or electrical engineering fields. Thus, a control algorithm which is appropriate to the structures having the abovementioned properties is needed for more effectively reducing the structural responses of the civil structures.

The time delay control (TDC) algorithm, which belongs to robust and adaptive control algorithms, might be one of the most suitable control algorithms for this purpose. It is not only simple and compact, but also very robust to unknown dynamics and disturbances. More than that, it is known that the TDC algorithm is especially powerful to a structure having slow dynamics. Even though it was first proposed in the field of mechanical engineering for motion control (Youcef-Toumi and Ito 1987a,b, 1988) and applied to robot manipulator, electrohydraulic servo system, DC servo motor system, and vibration isolation table (Hsia and Gao 1990, Chang *et al*. 1995, Chin *et al*. 1994, Chang and Lee 1994, Shin and Kim 2009, Sun and Kim 2012), the researches for vibration mitigation of large-scale structures such as buildings, bridges and towers using the TDC algorithm have not been done until Jang *et al*. (2014) numerically verified the feasibility of the TDC algorithm in the field of civil engineering. Still, its applicability to real structures is not guaranteed. Therefore, its applicability should be experimentally validated at least in a laboratory setting.

In this paper, the effectiveness and applicability of the TDC algorithm embedded AMD system is experimentally investigated. To this end, the theoretical background including the mathematical formulation of the control system is addressed first. And then, the performance of the proposed control system is thoroughly examined through a series of the experiments using a shaking table system with a small-scale three-story building structural model. After the experimental setup and the controller design, the free vibration and forced vibration tests are carried out, respectively. The test results of the proposed system are compared with those of the uncontrolled system in order to validate the effectiveness of the AMD system using the TDC algorithm.

2. Theoretical background

2.1 TDC algorithm

Let us consider a dynamic system in a general form, which can be either time invariant linear or time varying linear or nonlinear, described by

$$\dot{\mathbf{x}}(t) = \mathbf{f}(\mathbf{x}, t) + \mathbf{B}(\mathbf{x}, t)\mathbf{u}(t) + \mathbf{d}(t) \tag{1}$$

where $\mathbf{x}(t)$ is the plant state vector, $\mathbf{f}(\mathbf{x}, t)$ is the dynamics of the plant, $\mathbf{B}(\mathbf{x}, t)$ is the distribution matrix of the control input, and $\mathbf{d}(t)$ represents any kind of disturbance such as an external force. In Eq. (1), the plant dynamics, the distribution matrix of the control input and the

disturbance are assumed to be unknown. The objective of the TDC algorithm is to make the above system follow a reference model despite the presence of unknown dynamics and disturbances (Youcef-Toumi and Reddy 1992). A reference model with desirable dynamic characteristics is chosen as a stable time-invariant linear system as follows

$$\dot{\mathbf{x}}_{\mathbf{m}}(t) = \mathbf{A}_{\mathbf{m}}\,\mathbf{x}_{\mathbf{m}}(t) + \mathbf{B}_{\mathbf{m}}\,r(t) \tag{2}$$

where $\mathbf{x}_{\mathbf{m}}(t)$ is the state vector of the reference model, $\mathbf{A}_{\mathbf{m}}$ is the constant stable system matrix, $\mathbf{B}_{\mathbf{m}}$ is the constant command distribution matrix, and $r(t)$ is the command vector. The control input $\mathbf{u}(t)$ in Eq. (1) is determined such that the plant in Eq. (1) follows the reference model in Eq. (2); in other words, the difference between states of the plant and reference model (i.e., $\mathbf{e}(t) = \mathbf{x}_{\mathbf{m}}(t) - \mathbf{x}(t)$) to vanish according to the following error dynamic equation

$$\dot{\mathbf{e}}(t) = \mathbf{A}_{\mathbf{m}}\,\mathbf{e}(t) + \left[-\mathbf{f}(\mathbf{x},t) + \mathbf{A}_{\mathbf{m}}\,\mathbf{x}(t) + \mathbf{B}_{\mathbf{m}}\,r(t) - \mathbf{B}(\mathbf{x},t)\,\mathbf{u}(t) - \mathbf{d}(t)\right] = \mathbf{A}_{\mathbf{m}}\,\mathbf{e}(t) \tag{3}$$

Thus, the control input can be deduced from Eq. (3) as follows

$$\mathbf{u}(t) = \mathbf{B}^{+}\left[-\mathbf{f}(\mathbf{x},t) - \mathbf{d}(t) + \mathbf{A}_{\mathbf{m}}\,\mathbf{x}(t) + \mathbf{B}_{\mathbf{m}}\,r(t)\right] \tag{4}$$

where $\mathbf{B}^{+}\left(= (\mathbf{B}^{\mathrm{T}}\mathbf{B})^{-1}\mathbf{B}^{\mathrm{T}}\right)$ is the pseudo-inverse of the control input distribution matrix $\mathbf{B}(\mathbf{x}, t)$.

Because $\mathbf{B}(\mathbf{x}, t)$, $\mathbf{f}(\mathbf{x}, t)$ and $\mathbf{d}(t)$ in Eq. (4) are unknown, $\hat{\mathbf{B}}$ is used as an estimate of the $\mathbf{B}(\mathbf{x}, t)$ and it is assumed that $\mathbf{f}(\mathbf{x}, t)$ and $\mathbf{d}(t)$ have slow dynamic characteristics so that $\mathbf{f}(\mathbf{x}, t) + \mathbf{d}(t)$ can be replaced approximately with $\mathbf{f}(\mathbf{x}, t - \Delta t) + \mathbf{d}(t - \Delta t)$ for a small time delay Δt. Using Eq. (1), the estimate of $\mathbf{f}(\mathbf{x}, t) + \mathbf{d}(t)$ can be given by

$$\mathbf{f}(\mathbf{x}, t) + \mathbf{d}(t) \cong \mathbf{f}(\mathbf{x}, t - \Delta t) + \mathbf{d}(t - \Delta t) \cong \dot{\mathbf{x}}(t - \Delta t) - \hat{\mathbf{B}}\,\mathbf{u}(t - \Delta t) \tag{5}$$

By substituting Eq. (5) into Eq. (4), the control input by the TDC algorithm is obtained as follows

$$\mathbf{u}(t) = \mathbf{u}(t - \Delta t) + \hat{\mathbf{B}}^{+}\left\{-\dot{\mathbf{x}}(t - \Delta t) + \mathbf{A}_{\mathbf{m}}\,\mathbf{x}(t) + \mathbf{B}_{\mathbf{m}}\,r(t)\right\} \tag{6}$$

As seen in Eq. (6), all states and their first derivatives should be available to apply the TDC algorithm.

2.2 Derivation of the state-space equation for a building structure

Let us consider an n-DOF building structure model as shown in Fig. 1. It is assumed that only one active control system is implemented at the top floor and the responses only at the top floor of the structure can be available in view of practical situation.

Because the information of all states and their derivatives has to be available in order to apply the TDC algorithm as stated previously, the dynamics equation for structure should be written so that all states are acquirable.

The equation of motion can be described in the modal coordinate by

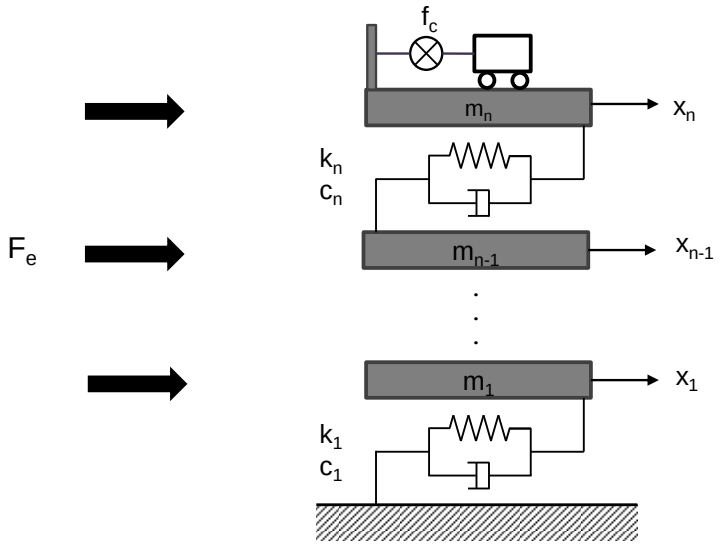

Fig. 1 n-DOF building structure

$$\overline{m}_j \ddot{q}_j + 2\xi_j \omega_j \dot{q}_j + \omega_j^2 q_j = f_c + \boldsymbol{\varphi}_j^T \mathbf{F_e}, \qquad j = 1 \sim n \tag{7}$$

where $\overline{m}_j = \boldsymbol{\varphi}_j^T \mathbf{M} \boldsymbol{\varphi}_j$ is the *j*th modal mass, ξ_j and ω_j are the *j*th damping ratio and natural frequency, respectively, f_c and $\mathbf{F_e}$ are the control force and the external force, respectively, and $\boldsymbol{\varphi}_j$ is the *j*th mode shape which is normalized so that $\boldsymbol{\varphi}_j(n) = 1$. Eq. (7) can be converted into the following state-space form

$$\begin{Bmatrix} \dot{q}_j(t) \\ \ddot{q}_j(t) \end{Bmatrix} = \begin{bmatrix} 0 & 1 \\ -\omega_j^2 & -2\xi_j\omega_j \end{bmatrix} \begin{Bmatrix} q_j(t) \\ \dot{q}_j(t) \end{Bmatrix} + \begin{bmatrix} 0 \\ 1/\overline{m}_j \end{bmatrix} f_c(t) + \begin{bmatrix} 0 \\ F_{ej} \left(= \dfrac{1}{\overline{m}_j} \boldsymbol{\varphi}_j^T \mathbf{F_e} \right) \end{bmatrix}, \quad j = 1 \sim n \tag{8}$$

By summing *n* equations of Eq. (8), we obtain

$$\begin{aligned} \sum_{j=1}^{n} \begin{Bmatrix} \dot{q}_j(t) \\ \ddot{q}_j(t) \end{Bmatrix} &= \sum_{j=1}^{n} \begin{bmatrix} 0 & 1 \\ -\omega_j^2 & -2\xi_j\omega_j \end{bmatrix} \begin{Bmatrix} q_j(t) \\ \dot{q}_j(t) \end{Bmatrix} + \sum_{j=1}^{n} \begin{bmatrix} 0 \\ 1/\overline{m}_j \end{bmatrix} f_c(t) + \sum_{j=1}^{n} \begin{bmatrix} 0 \\ F_{ej} \end{bmatrix} \\ &= \begin{bmatrix} \sum_{j=1}^{n} \dot{q}_j(t) \\ f\left(q_j(t),\, \dot{q}_j(t)\right) \end{bmatrix} + \begin{bmatrix} 0 \\ \sum_{j=1}^{n} 1/\overline{m}_j \end{bmatrix} f_c(t) + \begin{bmatrix} 0 \\ \sum_{j=1}^{n} F_{ej} \end{bmatrix} \end{aligned} \tag{9}$$

Since the mode shapes are normalized so that $\boldsymbol{\varphi}_j(n)=1$, the response at the top floor can be described by

$$x_n(t) = \sum_{j=1}^{n} \boldsymbol{\varphi}_j(n) q_j(t) = \sum_{j=1}^{n} q_j(t) \tag{10}$$

By substituting Eq. (10) into Eq. (9), we obtain the following state-space equation for a building structure in which the states and their derivatives are the responses at the top floor, which are assumed to be available

$$\begin{Bmatrix} \dot{x}_n(t) \\ \ddot{x}_n(t) \end{Bmatrix} = \begin{bmatrix} \dot{x}_n(t) \\ f\left(q_j(t), \dot{q}_j(t)\right) \end{bmatrix} + \begin{bmatrix} 0 \\ \sum_{j=1}^{n} 1/\overline{m}_j \end{bmatrix} f_c(t) + \begin{bmatrix} 0 \\ \sum_{j=1}^{n} F_{ej} \end{bmatrix} \tag{11}$$

2.3 Application of the TDC algorithm to structural control

As comparing Eq. (11) with Eq. (1), the control force $f_c(t)$ is obtained according to the TDC algorithm of Eq. (6) by

$$f_c(t) = f_c(t-\Delta t) + \hat{\mathbf{B}}^{+}\left[-\begin{Bmatrix} \dot{x}_n(t-\Delta t) \\ \ddot{x}_n(t-\Delta t) \end{Bmatrix} + \mathbf{A_m} \begin{Bmatrix} x_n(t) \\ \dot{x}_n(t) \end{Bmatrix} + \mathbf{B_m}\, r(t) \right] \tag{13}$$

where $\hat{\mathbf{B}} = \begin{bmatrix} 0 \\ \hat{b}_r \end{bmatrix}$ and $\hat{b}_r$ is the estimate of $\sum_{j=1}^{n} 1/\overline{m}_j$. The pseudo-inverse of $\hat{\mathbf{B}}$ is obtained by

$$\hat{\mathbf{B}}^{+} = \left(\begin{bmatrix} 0 & \hat{b}_r \end{bmatrix} \begin{bmatrix} 0 \\ \hat{b}_r \end{bmatrix} \right)^{-1} \begin{bmatrix} 0 & \hat{b}_r \end{bmatrix} = \begin{bmatrix} 0 & \dfrac{1}{\hat{b}_r} \end{bmatrix} \tag{14}$$

Because the control objective of structural control is to mitigate the vibration of a structure, the command term $r(t)$ is set to zero. And let us define the system matrix of the reference model $\mathbf{A_m}$ as follows

$$\mathbf{A_m} = \begin{bmatrix} 0 & 1 \\ -\omega_m^2 & -2\xi_m\omega_m \end{bmatrix} \tag{15}$$

where ω_m and ξ_m are the natural frequency and damping ratio of the reference model, respectively. By substituting Eqs. (14) and (15) into Eq. (13), it can be rewritten by

$$f_c(t) = f_c(t-\Delta t) + \frac{1}{\hat{b}_r}\left[-\ddot{x}_n(t-\Delta t) - \omega_m^2 x_n(t) - 2\xi_m \omega_m \dot{x}_n(t) \right] \tag{16}$$

As seen in Eq. (16), the design parameters are $\hat{b}_r$, the estimate of $\sum_{j=1}^{n} 1/\overline{m}_j$ and dynamic characteristics of reference model, ω_m and ξ_m. And all states and their first derivatives should be available to apply the TDC algorithm. Among the design parameters, $\hat{b}_r$ is related with the stability of the control system, and the inequality condition for guaranteeing the stability was derived as follows (Jang *et al*. 2014)

$$\hat{b}_r > \frac{1}{2} b_r \tag{17}$$

3. Experimental test results

3.1 Experimental setup

To investigate the feasibility and control performance of the TDC algorithm in mitigating the excessive vibration of a building a series of experimental tests were conducted by using a shaking table uniaxially driven by a servo-controlled hydraulic actuator in the Structural Control and Intelligent Systems Laboratory (SCaIS) at KAIST. The shaking table has a testing platform of 110 cm by 96 cm, a maximum payload of 600 kg, a maximum acceleration of ±0.4 g and a maximum velocity of 21 cm/s. The hydraulic actuator with the maximum dynamic force of 2 tons and the stroke length of ±5 cm can be controlled by a servo-hydraulic controller in a displacement or acceleration feedback mode. A schematic of the experimental setup is shown in Fig. 2.

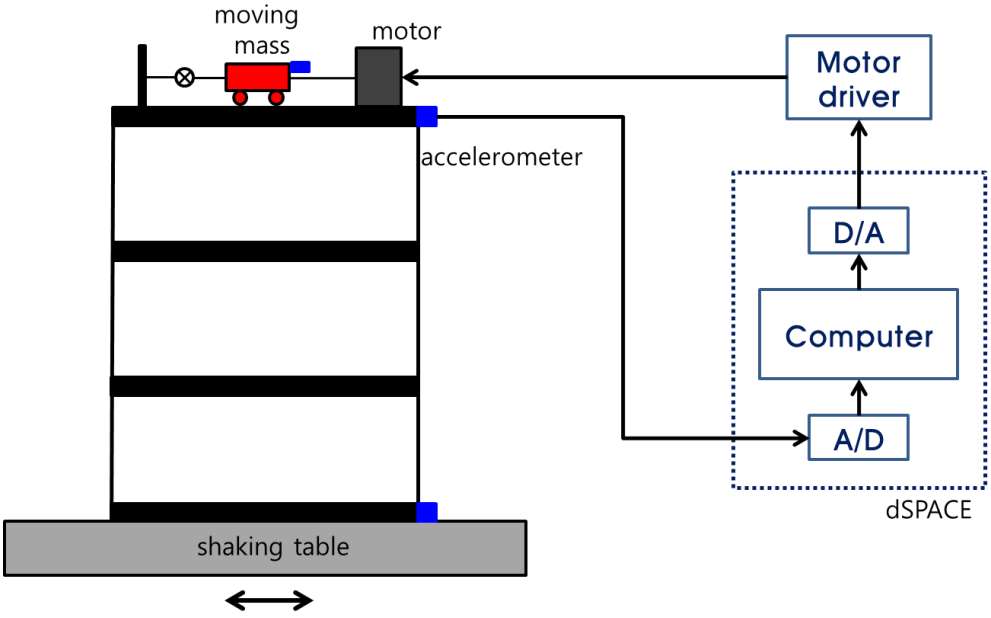

Fig. 2 Schematic of experimental setup

Fig. 3 Scaled 3-story shear building model

The test structure model used in the experiment is a scaled 3-story shear building model as shown in Fig. 3. The columns are constructed of aluminum and the total height is 1050 mm, and the floor masses are constructed of steel and the total weights are 48.27 kg, which is distributed evenly in each floor. The dynamic characteristics of the structure model were identified by a frequency-domain system identification technique. Fig. 4 shows representative magnitude and phase plots for the experimentally determined and analytically estimated frequency response functions (FRFs). The identified modal masses are 30, 43 and 160 kg, natural frequencies are 2.145, 6.595 and 10.531 Hz, and damping ratios are 0.26, 0.7 and 0.4%.

The AMD system shown in Fig. 5 which provides the control force to the structure consists of a moving mass, an LM guide rail, a ball screw, a timing belt and a servo motor (model: Mitsubishi HP-KP23 200W). The rotary motion of the servo motor delivered to the ball screw and it converts the rotary motion into rectilinear motion of the moving mass, which is driven on the LM guide rail. The motion of the moving mass generates the inertia force, and it is utilized as the control force for the structure. In order to induce the accurate inertia force by the moving mass, the dynamics of the AMD system should be considered. In the experiments, an inverse transfer function of the acceleration of the moving mass with respect to the command voltage into the servo motor driver is constructed and implemented in the control signal processing in order to compensate the dynamics of the AMD system. Fig. 6 presents the magnitude and phase plots for the experimentally determined and analytically estimated FRFs of the acceleration of the moving mass with respect to the command voltage of the AMD system, where the estimated FRF is determined using MATLAB/System Identification Toolbox in the discrete time-domain as follows

$$\hat{H}_{u\ddot{a}}(z) = \frac{1832.1\, z^{-1} - 1756.5\, z^{-2}}{1 - 1.6019\, z^{-1} + 0.71839\, z^{-2}} \tag{18}$$

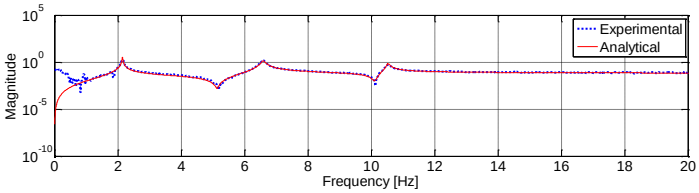

(a) Magnitude

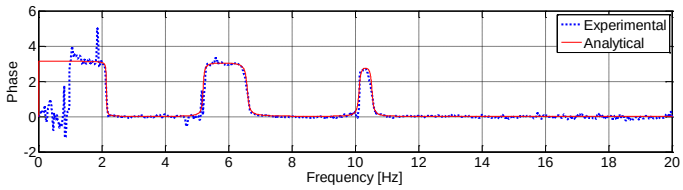

(b) Phase

Fig. 4 FRF from relative AMD acceleration to third floor acceleration

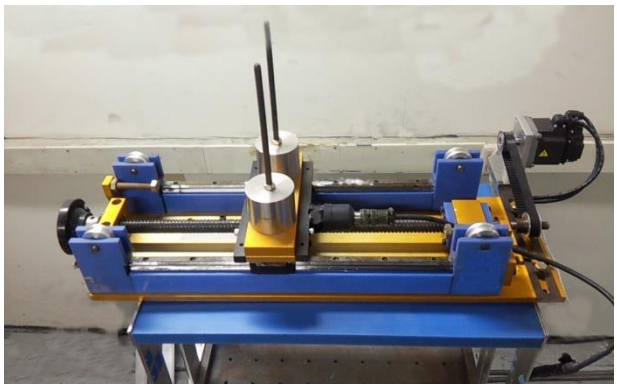

Fig. 5 Active mass damper system

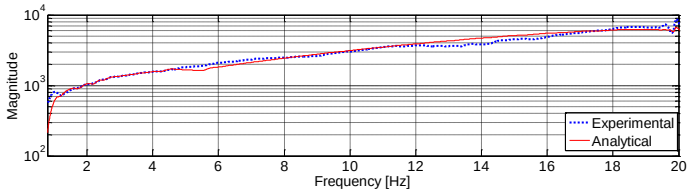

(a) Magnitude

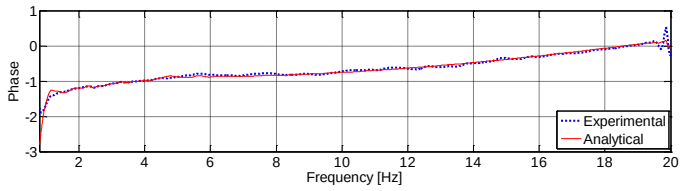

(b) Phase

Fig. 6 FRF from AMD command voltage to AMD acceleration

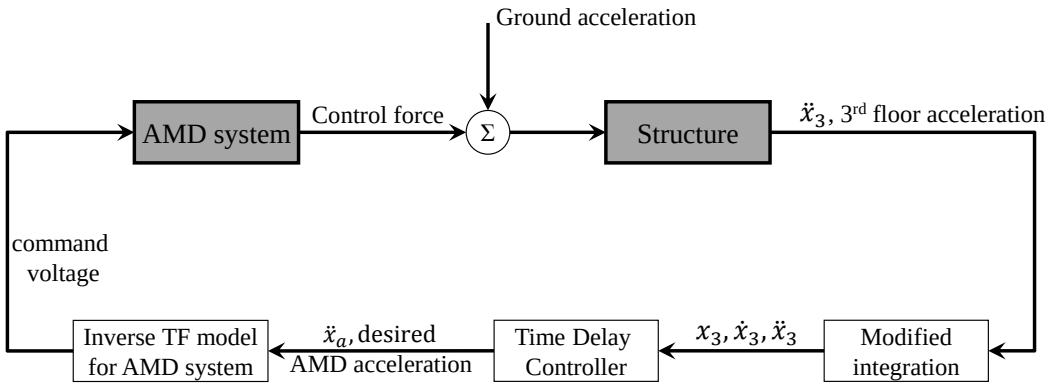

Fig. 7 Block diagram of the experiments for structural control using the TDC algorithm

The voltage into the servo motor of the AMD system was processed by dSPACE ControlDesk and Simulink of MatLab in a personal computer. The voltage calculated in the computer was supplied to the servo motor driver (model: Mitsubishi MR-J3-20A) by dSPACE Model ds1104 and the measured acceleration of the structure model is digitized also by the ds1104.

In the experiments, the acceleration at the third floor of the structure model was measured by an accelerometer (model: PCB 393B12) and it is used for calculating the required control force by the TDC algorithm. Besides, the accelerations of the shaking table platform and the moving mass of the AMD system were measured to check out the results. A block diagram for the whole closed-loop system is shown in Fig. 7, where the plant consists of the structure model and the AMD system.

As stated previously, all state variables and its first derivatives (i.e., displacement, velocity and acceleration of the structure model) should be available to apply the TDC algorithm. However, since only the acceleration is measured in practice, a numerical integrator or state estimator must be used to obtain the velocity and displacement. In this experiment, a numerical integration is used in order to avoid the difficulties in identifying the structure model, which is required to use the state estimator. However, the ideal integration method accumulates even a small DC-offset value measured acceleration; thus, a modified integration (Zhu 2004) is applied, which can remove the accumulation of the DC offset. The modified integrator is just a slight variation of the ideal integrator as follows

$$\frac{1}{s} : \text{ideal integrator} \quad \Rightarrow \quad \frac{1}{s+a} : \text{modified intgrator} \tag{19}$$

where s is Laplace operator. By using the modified integrator, the integration of the low frequency components converges to zero. The parameter a, which is referred as cut-off frequency of a first order system, affects distortion of the phase and magnitude of the signal. As a rule of thumb, the value of a is chosen as about 1/10 of the lowest frequency of interest. In this study, it is determined as 0.05 by considering the dynamic range of the accelerometer (> 0.5 Hz).

3.2 Controller design

The design parameters in the TDC algorithm are the dynamic characteristics of the reference model and the estimate of the input distribution matrix. The reference model, which is denoted by $\mathbf{A_m}$ in Eq. (15), is a target system which has to be achieved by the TDC algorithm; therefore, it should be selected as a stable system. In this experiment, the natural frequency and the damping ratio of the reference model were chosen as 0.1 Hz and the critical (i.e., $\xi_m = 1$), respectively.

The estimate of the input distribution matrix, which is denoted by $\hat{b}_r$ in Eq. (16), should be chosen by considering the inequality condition of Eq. (17) for guaranteeing the stability of the control system. As presented in Eq. (13), $b_r = \sum_{j=1}^{n} 1/\overline{m}_j$, where $\overline{m}_j = \boldsymbol{\varphi}_j^T \mathbf{M} \boldsymbol{\varphi}_j$ is the *j*-th modal mass. Because it is assumed that the exact values of the modal masses are unknown, the guideline for the determination of $\hat{b}_r$ is required. Because mode shapes are normalized such that $\boldsymbol{\varphi}_j(n) = 1$, the first modal mass, $\overline{\mathrm{m}}_1$, is the smallest among the modal masses. Therefore, the following inequality can be derived

$$b_r = \sum_{j=1}^{n} \frac{1}{\overline{m}_j} < \frac{n}{\overline{m}_1} < \frac{n}{m_n} \tag{20}$$

where m_n denotes the mass of the *n*-th floor. Thus, if we choose $\hat{b}_r$ larger than $\frac{n}{m_n}$, then the stability condition of Eq. (17) is satisfied obviously. The mass of the *n*-th floor, m_n, can be assumed easily, and it does not need to be exact.

At the test structure model, the number of floor is 3 and the mass of the 3rd floor is about 16 kg; thus the estimate $\hat{b}_r$ can be chosen larger than 0.2. In this experiment, $\hat{b}_r = 1.66$ is chosen by considering the maximum AMD stroke.

3.3 Free vibration test

At first, the free vibration test was performed to check an increase in the equivalent damping ratio of the structure model, because it is one of the simplest ways to verify the control performance. Fig. 8 shows the acceleration at the third floor of the structure model and the command voltage of the AMD system for the case of the excitation at the first natural frequency. The structure model was excited as a harmonic motion of the first mode by the AMD system, and then the AMD system was stopped in uncontrolled mode or operated by the TDC algorithm in the control mode.

As shown in Fig. 8, the free vibration response in the controlled case decays out much faster than in the uncontrolled case. It can be easily observed from the two shaded regions in the figure. The equivalent damping ratios can be calculated from the free vibration responses by using the logarithmic decrement method. The damping ratio in the uncontrolled case is 0.26%; on the other hand, the ratio in the controlled case is 6.0%. The damping ratio is increased over than 20 times. It is, therefore, said that the proposed control system can effectively mitigate the free vibration response of the building structure.

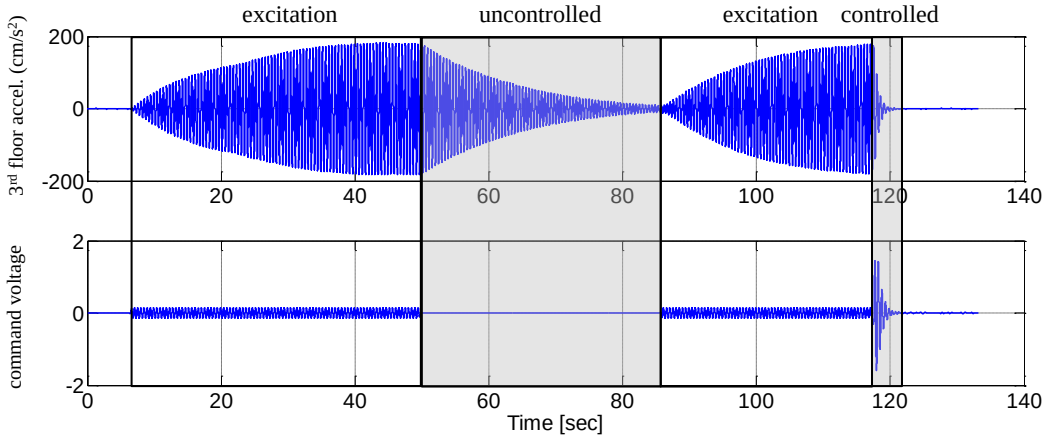

Fig. 8 Free vibration test result

3.4 Forced vibration test

As the inputs to the structure model, the band-limited white noise and two different historical earthquakes were used. The ground accelerations considered herein are

1) Artificially generated white noise ground acceleration which is uniformly distributed in the frequency range of 0-20 Hz;

2) El Centro earthquake (The N-S component recorded at the Imperial Valley Irrigation District substation in El Centro, California, during Imperial Valley, California earthquake, May 18, 1940) scaled to 10% amplitude and 2 times the recorded rate; and

3) Hachinohe earthquake (The N-S component recorded at Hachinohe City during the Tokachi-oki earthquake, May 16, 1968) scaled 15% amplitude and 2 times the recorded rate.

Fig. 9 shows the time histories of the third floor acceleration in the three different values of $\hat{b}_r$ under the 0-20Hz band-limited white noise. As seen from the figures, the acceleration response can be more effectively mitigated with a small value of $\hat{b}_r$. The results of the experiments are briefly summarized in Table 1. In the table, the values in the parentheses denote % reduction of the responses in the controlled case compared to those in the uncontrolled case. By contrast to the control performance, it is shown that a more control force, which is the inertia force of the AMD moving mass, is required as $\hat{b}_r$ being smaller.

Fig. 10 presents the experimental result under the band-limited white noise and $\hat{b}_r$ =1.66, in which (a) time history of the ground acceleration, (b) time history of the acceleration at the third floor, (c) the desired and measured AMD acceleration, and (d) FRF of the third floor acceleration. The overall maximum and RMS responses are reduced by 44.52% and 66.42%, respectively. It is demonstrated from the test results that the measured relative AMD acceleration agrees well with the desired one as presented in Fig. 10(c), which means the motion of the moving mass of the AMD follows the desired trajectory well, and consequently the proper control force is applied to the structure, resulting in the good control performance of the proposed control system.

Table 1 Experimental results under the band-limited white noise

Case	Uncontrolled	Controlled	
Maximum acceleration (cm/s^2)	30.75	$\hat{b}_r = 1.66$	17.06 (-44.52%)
		$\hat{b}_r = 3.32$	20.04 (-34.83%)
		$\hat{b}_r = 6.64$	21.99 (-28.48%)
RMS acceleration (cm/s^2)	8.88	$\hat{b}_r = 1.66$	2.98 (-66.42%)
		$\hat{b}_r = 3.32$	3.79 (-57.33%)
		$\hat{b}_r = 6.64$	4.76 (-46.42%)
Maximum control force (N)	-	$\hat{b}_r = 1.66$	1.90
		$\hat{b}_r = 3.32$	1.34
		$\hat{b}_r = 6.64$	0.86

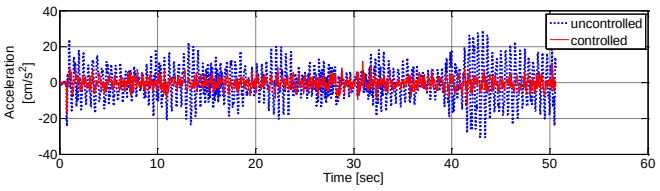

(a) $\hat{b}_r = 1.66$

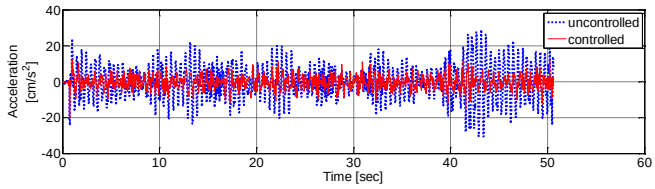

(b) $\hat{b}_r = 3.32$

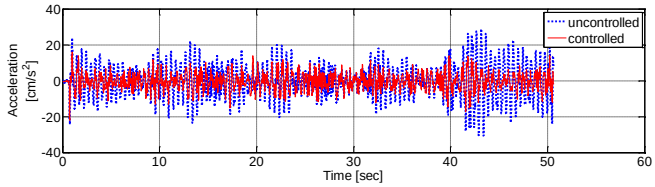

(c) $\hat{b}_r = 6.64$

Fig. 9 Acceleration responses at the third floor under the 0-20 Hz band-limited white noise with the different values of $\hat{b}_r$

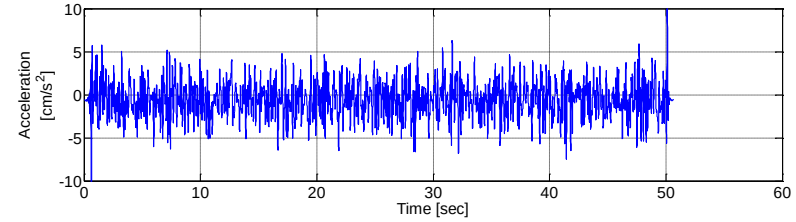

(a) Ground acceleration

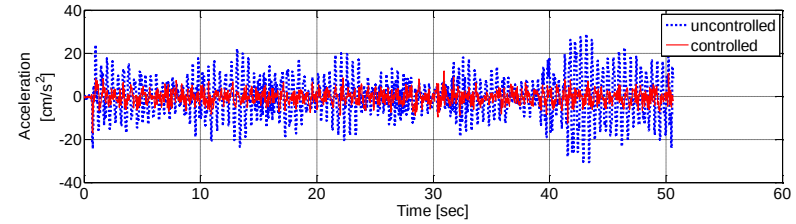

(b) Third floor acceleration

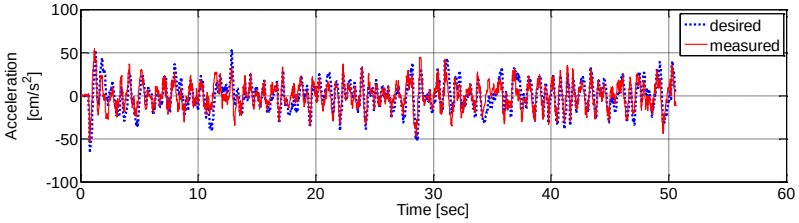

(c) Relative AMD acceleration

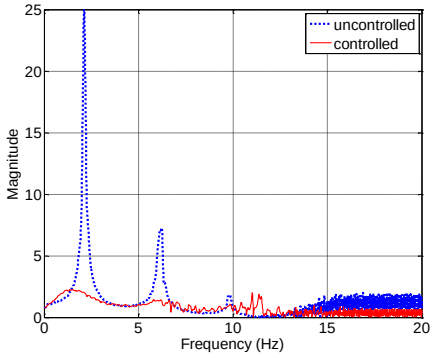

(d) FRF of the third floor acceleration

Fig. 10 Experimental results under the 0-20 Hz band-limited white noise

Figs. 11 and 12 present the experimental results under the scaled El Centro earthquake and Hachinohe earthquake, respectively, in which (a) time history of the ground acceleration, (b) time history of the acceleration at the third floor, (c) the desired and measured AMD acceleration, and (d) FRF of the third floor acceleration. As seen from Figs. 11(b), 11(d) and 12(b), 12(d), compared to the uncontrolled case, the third floor acceleration response is reduced significantly by the controlled system. The overall maximum and RMS of the third floor acceleration are reduced from 119.9 cm^2/sec (uncontrolled) to 89.3 cm^2/sec (controlled) and 44.7 cm^2/sec to 14.3 cm^2/sec under

the scaled El Centro earthquake, and from 201.5 cm^2/sec (uncontrolled) to 107.6 cm^2/sec (controlled) and 65.9 cm^2/sec to 19.3 cm^2/sec under the scaled Hachinohe earthquake. The motion of the moving mass of the AMD follows the trajectory well as shown in Figs. 11(c) and 12(c). In summary, it can be said that the proposed control system significantly reduces the structural response under the several different seismic loadings.

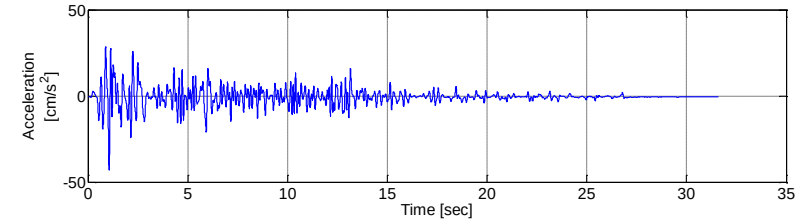

(a) Ground acceleration

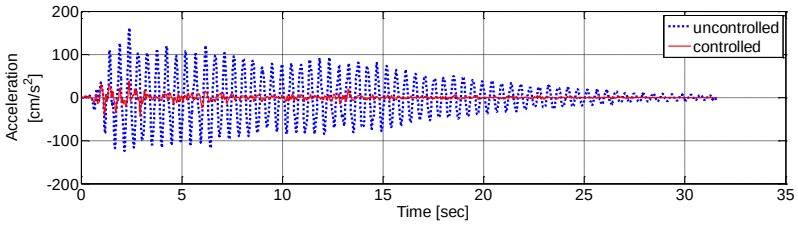

(b) Third floor acceleration

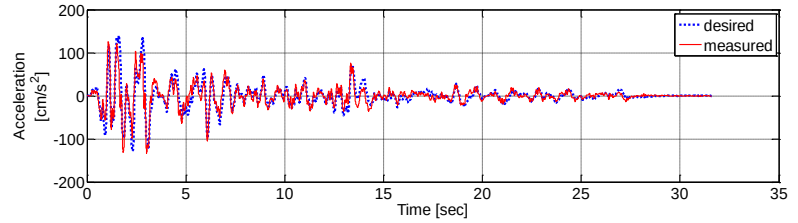

(c) Relative AMD acceleration

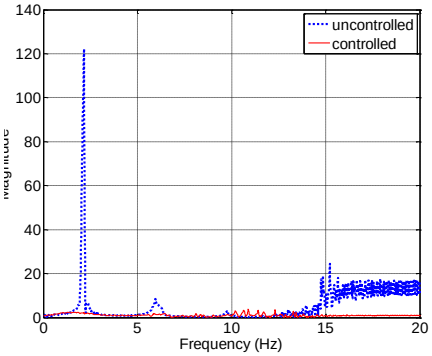

(d) FRF of the third floor acceleration

Fig. 11 Experimental results under the scaled El Centro earthquake

Table 2 Experimental results under the scaled earthquakes (unit: cm/s^2)

Case		Uncontrolled	Controlled
The scaled El Centro earthquake	Max. acceleration	161.22	43.73 (-72.87%)
	RMS acceleration	45.28	5.82 (-87.14%)
The scaled Hachinohe earthquake	Max. acceleration	194.99	68.82 (-64.71%)
	RMS acceleration	57.83	6.50 (-88.76%)

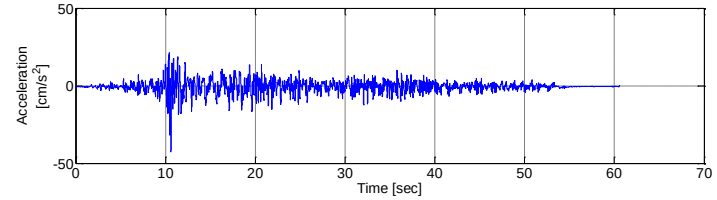

(a) Ground acceleration

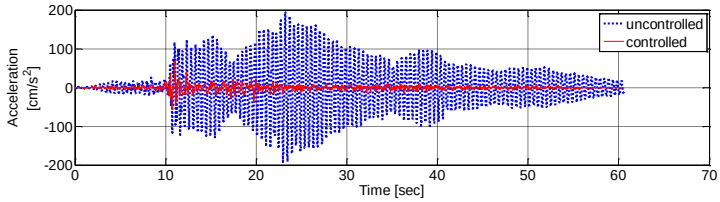

(b) Third floor acceleration

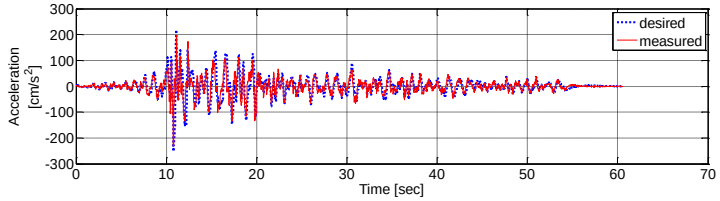

(c) Relative AMD acceleration

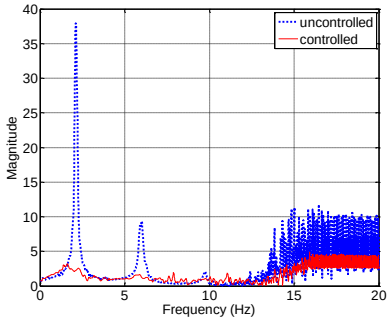

(d) FRF of the third floor acceleration

Fig. 12 Experimental results under the scaled Hachinohe earthquake

3.5 Discussion

As experimentally demonstrated in the preceding two sections, the proposed TDC algorithm could be effective to mitigate the excessive vibration of a building structure. At this section, a few issues related to the control performance and robustness of the TDC algorithm are discussed in more detail.

First, the control performance of the TDC algorithm is examined by comparing with the results of the experimental study conducted by other researchers. Dyke *et al*. (1996) developed the H_2/LQG control algorithm to reduce the vibration of the three-story building model equipped with the AMD system on the top floor subjected to the base excitation. This is exactly the same experimental setup as in this study. According their test results, the LQG control algorithm reduced the maximum acceleration at the third floor by 65% under the El Centro earthquake compared to the uncontrolled case. On the other hand, the proposed TDC algorithm has the 72% reduction under the same base excitation (see Table 2). Based on this comparison, it can be said that the control performance of the TDC algorithm is comparable to that of the LQG control algorithm.

During the design process of the TDC algorithm, decision of $\hat{b}_r$ in Eq. (16) is the most important step because it is related to the stability as well as the control performance of the control system. Eq. (17) means the inequality condition for guaranteeing the stability of the control system, and Eq. (20) shows the guideline to satisfy Eq. (17). The robustness of the control performance with respect to $\hat{b}_r$ was numerically examined in Jang *et al*. (2014). Also, according to Table 1 at Section 3.4, it is experimentally demonstrated that the TDC algorithm maintains the good control performance with the different values of $\hat{b}_r$. Moreover, it is well known that the TDC algorithm has the excellent robustness properties to unknown system dynamics and disturbances (Youcef-Toumi and Ito 1987a, b, 1988).

4. Conclusions

In this paper, the effectiveness and applicability of the time delay control (TDC) algorithm for an active mass damper (AMD) system to mitigate the excessive vibration of a building structure was experimentally investigated. First, the theoretical background including the mathematical formulation of the control system was described. And then, an experimental study using a shaking table system with a small-scale three-story building structural model was thoroughly carried out. In the experimental tests, the control performance of the proposed control system was examined by comparing its structural responses with those of the uncontrolled system in the cases of forced vibration as well as free vibration. The test results showed that the TDC algorithm embedded AMD system significantly reduced the structural response of the test model. Therefore, it is concluded that the proposed control system can be an effective means for mitigating the excessive vibration of a building structure.

Acknowledgements

This research was supported by a grant(14RTRP-B072484-02) from Railroad Technology Research Program funded by Ministry of Land, Infrastructure and Transport(MOLIT) of Korea government and Korea Agency for Infrastructure Technology Advancement (KAIA).

References

Chang, P.H. and Lee, J.W. (1994), "An observer design for time-delay control and its application to dc servo motor", *Control Eng. Pract.*, **2**(2), 263-270.

Chang, P.H., Kim, D.S. and Park K.C. (1995), "Robust force/position control of a robot manipulator using time-delay control", *Control Eng. Pract.*, **3**(9), 1255-1264.

Chin, S.M., Lee, C.O. and Chang, P.H. (1994), "An experimental study on the position control of an electrohydraulic servo system using time delay control", *Control Eng. Pract.*, **2**(1), 41-48.

Datta, T.K. (2001), "A state-of-the-art review on active control of structures", *J. Earthq. Technol. - ISET*, **40**(1), 1-17.

Dyke, S.J., Spencer, Jr., B.F., Quast, P., Kaspari, Jr. D.C. and Sain, M.K. (1996), "Implementation of an active mass driver using acceleration feedback control", *Microcomput. Civil Eng.*, **11**, 305-323.

Hsia, T.C. and Gao, L.S. (1990), "Robot manipulator control using decentralized linear time-invariant time-delayed controllers", *Proceedings of the IEEE International Conference on Robotics and Automation*, Cincinnati, OH, May.

Jang, D.D., Jung, H.J. and Moon, Y.J. (2014), "Active mass damper system using time delay control algorithm for building structure with unknown dynamics", *Smart Struct. Syst.*, **13**(2), 305-318.

Kobori, T., Koshika, N., Yamada, K. and Ikeda, Y. (1991a), "Seismic-response-controlled structure with active mass driver system. Part 1: Design", *Earthq. Eng. Struct. D.*, **20**(1), 133-149.

Kobori, T., Koshika, N., Yamada, K. and Ikeda, Y. (1991b), "Seismic-response-controlled structure with active mass driver system. Part 2: Verification", *Earthq. Eng. Struct. D.*, **20**(1), 151-166.

Nishitani, A. and Inoue, Y. (2001), "Overview of the application of active/semiactive control to building structures in Japan", *Earthq. Eng. Struct. D.*, **30**(11), 1565-1574.

Pourzeynali, S., Lavasani, H.H. and Modarayi, A.H. (2007), "Active control of high rise building structures using fuzzy logic and genetic algorithms", *Eng. Struct.*, **29**(3), 346-357.

Shin, Y.H. and Kim, K.J. (2009), "Performance enhancement of pneumatic vibration isolation tables in low frequency range by time delay control", *J. Sound Vib.*, **321**(3-5), 537-553.

Spencer, Jr., B.F. and Nagarajaiah, S. (2003), "State of the art of structural control", *J. Struct. Eng.* - ASCE, **129**(7), 845-856.

Sun, J.O. and Kim, K.J. (2012), "Six-degree of freedom active pneumatic table based on time delay control technique", *Proceedings of the Institution of Mechanical Engineers, Part 1; Journal of System and Control Engineering*, **226**(5), 638-650.

Youcef-Toumi, K. and Ito. O. (1987a), "Controller design for systems with unknown nonlinear dynamics", *Proceedings of the American Control Conference*, Minneapolis, MN, June, 836-845.

Youcef-Toumi, K. and Ito, O. (1987b), "Model reference control using time delay for nonlinear plants with unknown dynamics", *Proceedings of the 10th Triennial World Congress of International Federation of Automatic Control World Congress*, Munich, Germany, July.

Youcef-Toumi, K. and Ito. O. (1988), "A time delay controller for systems with unknown dynamics", *Proceedings of the American Control Conference*, Atlanta, GA, June.

Youcef-Toumi, K. and Reddy, S. (1992), "Analysis of linear time invariant systems with time delay", *J. Dynam. Syst. Measurement Control*, **114**(4), 544-555.

Zhu, W.H. (2004), "On active acceleration control of vibration isolation systems", *Proceedings of the 43rd IEEE Conference on Decision and Control*, Atlantis, Paradise Island, Bahamas.